Transport by capillary waves: Fluctuating Stokes drift

O. N. Mesquita,* S. Kane, and J. P. Gollub
Physics Department, Haverford College, Haverford, Pennsylvania 19041
and Physics Department, University of Pennsylvania, Philadelphia, Pennsylvania 19104
(Received 19 August 1991)

Measurements of dye transport by *disordered* capillary waves (generated by the Faraday instability) are reported as a function of the wave amplitude. The transport is diffusive, with effective diffusion coefficients that are typically at least a factor of 10^3 larger than the molecular values. A model based on fluctuations in the Stokes drift caused by the disordered surface waves is tested and found to predict diffusion coefficients of the right order of magnitude, but roughly a factor of 3 too small. Residual correlations in the wave field are suggested to account for this discrepancy.

PACS number(s): 47.35.+i, 47.20.−k

I. INTRODUCTION

Many of the characteristic phenomena of nonlinear systems, including pattern formation and spatiotemporal chaos, are exhibited by parametrically forced standing waves on fluid surfaces. These waves are generated by vertical oscillation of a container partially filled with fluid. At a critical driving amplitude, a parametric instability leads to standing surface waves at half the forcing frequency.

Extensive experimental and theoretical studies have been carried out in order to understand the nonlinear dynamical properties of these "Faraday waves," and several reviews have appeared [1–3]. One important property is the transition from a spatially periodic and steady wave pattern to a disordered and fluctuating state as the driving amplitude is increased. The correlation length and correlation time were found to decrease sharply at this order-disorder transition [4].

Increasing attention has been given recently to the phenomena of stirring, mixing, and transport in hydrodynamic systems [5]. The problem of understanding transport by surface waves has a long history. Ramshankar *et al.* [6] recently examined this problem experimentally by studying the transport of passive tracers on surface waves generated by the Faraday instability, both in the ordered but weakly modulated regime and in the disordered regime. They found substantial transport and mixing in both cases, and studied the statistical properties of the motion of both individual particles and patches of dye. In the disordered regime, the transport was found to be "diffusive," in the sense that the mean-square displacement of particles or fluid elements increased linearly with time, with effective diffusion coefficients of the order of 0.1 cm^2/s, roughly 10^4 times larger than the molecular diffusion coefficient of dye molecules. The weakly modulated case, on the other hand, was found to be "superdiffusive," meaning that displacements increased faster than linearly with time. Aranson *et al.* [7] have recently attempted to describe the transport in this regime qualitatively, by constructing a model of chaotic advection based on two orthogonal wave trains that are modulated in space and time. Though no quantitative comparison with experiment has been made, these authors did note a superdiffusive regime for certain choices of the modulation parameters.

In this paper we compare the measured transport coefficients in the *disordered* regime with a quantitative model of dispersion. The model, originally proposed by Herterich and Hasselmann [8] in the context of ocean-wave transport, is based on an analysis of the fluctuating Stokes-drift current, a small net transport that is quadratic in the wave amplitude. The Stokes drift should be a fluctuating quantity in a disordered wave field, and these fluctuations should lead to transport and dispersion of tracers. The model does not have adjustable parameters and provides absolute predictions, provided that the spatial power spectrum of the wave field and the mean-square wave amplitude are known. We find that the model predicts effective diffusion coefficients that are of the right order of magnitude, but somewhat smaller than the observed values. Possible reasons for the difference, which decreases as the waves become more disordered, are discussed at the end of the paper.

II. FLUCTUATING STOKES DRIFT MODEL OF TRANSPORT

Because particle trajectories are not quite closed for traveling waves, a net time-averaged drift current in the direction of propagation of the waves (quadratic in the wave amplitude) is experienced by fluid elements or tracer particles that follow them. For sinusoidal traveling surface waves in the xy plane, the Stokes drift velocity $\mathbf{u}_S$ is given by [9]

$$\mathbf{u}_S(z)=2\mathbf{k}\omega\langle h^2\rangle e^{2kz}\ , \tag{1}$$

where $\mathbf{k}$, ω, and $\langle h^2\rangle$ are the wave vector, angular frequency, and mean-square surface displacement of the wave, respectively. Here z is the vertical coordinate measured from the mean free surface and is negative below the surface. Equation (1) is valid in the deep-water limit, where the depth of the fluid is much greater than the wavelength of the surface waves.

In the case of standing waves composed of two oppositely directed waves with equal amplitudes, the net Stokes-drift velocity will vanish. Therefore, for pure standing waves no transport of particles would be expected (other than that caused by molecular diffusion). However, in a disordered wave field the local drift velocities induced by the various fluctuating wave components will not sum to zero at each instant; the resulting irregular fluctuations in the local Stokes drift will cause a fluid or tracer particle to follow a path resembling a random walk. Though such a model seems possibly appropriate for surface waves generated by the Faraday instability in the disordered regime, a quantitative test is needed.

To obtain a quantitative theoretical prediction, we apply the method proposed by Herterich and Hasselmann [8]. For a random-wave field the ensemble-averaged Stokes drift is given by

$$\langle \mathbf{u}_S(z) \rangle = 2 \int F(\mathbf{k}) \omega \mathbf{k} e^{2kz} d^2k \ , \tag{2}$$

where the two-dimensional wave spectrum $F(\mathbf{k})$ is normalized to the mean-square surface displacement

$$\int F(\mathbf{k}) d^2k = \langle h^2 \rangle \ . \tag{3}$$

From the theory of Brownian motion, a particle whose velocity components $u_i(t)$ $(i=1,2)$ undergo statistically stationary fluctuations generally follows a random walk in each coordinate, such that

$$\langle (x_i - \langle x_i \rangle)(x_j - \langle x_j \rangle) \rangle = 2 D_{ij} t \ , \tag{4}$$

where the diffusivity tensor D_{ij} is given by the time integral of the correlation function of the velocity fluctuations $\delta u_i = u_i - \langle u_i \rangle$:

$$D_{ij} = \tfrac{1}{2} \int_{-\infty}^{\infty} \langle \delta u_i(t+\tau) \delta u_j(t) \rangle d\tau \ . \tag{5}$$

To determine the velocities, Herterich and Hasselmann began with a linear approximation of the random-wave field as a superposition of an ensemble of statistically independent, normally distributed gravity-wave components. The nonlinear wave field was then constructed by a perturbation expansion with respect to these wave amplitudes, an approach that is well established in the wave literature. Their method can be applied directly to capillary waves by substituting the corresponding dispersion relation in their computation. This leads by straightforward methods to the following expression for the diffusion tensor for surface transport in terms of the wave-vector spectrum $F(k,\theta)$ expressed in circular coordinates:

$$\begin{bmatrix} D_{xx} & D_{xy} \\ D_{yx} & D_{yy} \end{bmatrix} = \left[\frac{\pi}{6} \right] \left[\frac{T}{\rho} \right]^{1/2} \langle h^2 \rangle^2 \overleftrightarrow{\mathrm{Q}} \ , \tag{6}$$

where the integral $\overleftrightarrow{\mathrm{Q}}$ involves the wave-number spectrum and is given by

$$\overleftrightarrow{\mathrm{Q}} = \frac{\int \int \int dk \, d\theta_1 d\theta_2 k^{6.5} F(k,\theta_1) F(k,\theta_2) [1+\cos(\theta_2-\theta_1)]^2 \overleftrightarrow{\mathrm{M}}}{\left[\int \int dk \, d\theta \, dF(k,\theta) \right]^2} \ , \tag{7}$$

and the matrix $\overleftrightarrow{\mathrm{M}}$ contains angular factors that are different for the four components D_{ij} of the effective-diffusion matrix

$$\overleftrightarrow{\mathrm{M}} = \begin{bmatrix} (\cos\theta_1 + \cos\theta_2)^2 & (\sin\theta_1 + \sin\theta_2)(\cos\theta_1 + \cos\theta_2) \\ (\sin\theta_1 + \sin\theta_2)(\cos\theta_1 + \cos\theta_2) & (\sin\theta_1 + \sin\theta_2)^2 \end{bmatrix} \ . \tag{8}$$

In Eq. (6), T is the surface tension and ρ the density of the fluid. Since the Stokes-drift velocity decays exponentially with depth, this estimate is valid only in a thin surface layer. Note that if $F(k,\theta)$ is fixed, the diffusion tensor is predicted to be proportional to $\langle h^2 \rangle^2$, so that it is highly nonlinear in the rms wave amplitude.

It is instructive to make an order-of-magnitude estimate for D_{ij} as predicted by the fluctuating Stokes-drift model by first assuming that the spectrum of the surface displacements is isotropic, i.e., $F(k,\theta)=F(k)$, and that it consists of a narrow peak (with linewidth Δk) centered around k_0. In addition, we assume a rectangular line shape such that

$$F(k) = \frac{\langle h^2 \rangle}{2\pi k_0 \Delta k} \tag{9}$$

over a bandwidth Δk, so that Eq. (3) is satisfied. Using this $F(k)$ in Eq. (7), one finds that the off-diagonal diffusion coefficients D_{xy} and D_{yx} vanish, while the diagonal terms turn out to be

$$D_{xx} = D_{yy} = \frac{5\pi}{12} \left[\frac{T}{\rho} \right]^{1/2} \frac{k_0^{4.5}}{\Delta k} (\langle h^2 \rangle)^2 \ . \tag{10}$$

From the sample calculation above we see that the diffusion coefficient depends strongly on the wave amplitude, but not so strongly on the linewidth of the spectrum of surface displacements. For an order-of-magnitude estimate, we use parameters appropriate for the air-water surface at 25 °C: $T=73$ dyn/cm; $\rho=1.0$ g/cm^3; $k_0=24$ cm^{-1} (for waves oscillating at 160 Hz); $\langle h^2 \rangle \approx 10^{-4}$ cm^2; and $\Delta k / k \approx 0.3$. We obtain from Eq. (10) an estimate for the effective diffusivity of 0.3 cm^2/s, which comes close to the experimental values.

For a quantitative test of the theory, we measure both $F(k,\theta)$ and $\langle h^2 \rangle$ to obtain a "calculated" diffusion coefficient D_c (anticipating that it will turn out to be nearly isotropic), using Eqs. (6)–(8). It is not a strictly theoretical quantity because it depends on the measured

spectral distribution. We also measure the diffusion coefficient D_m of the spreading dye as a function of driving amplitude, and then compare D_c with the measured value D_m.

III. EXPERIMENTAL MEASUREMENTS

All the experiments to be described are conducted in a square Plexiglas cell of dimensions $8\times8\times2$ cm, partially filled to a depth of 1.5 cm with deionized water. The cell is mounted on a precision electromagnetic shaker driven by a frequency synthesizer and power amplifier, as described in Ref. [6]. Excitation amplitudes larger than a critical value A_c at an excitation frequency of 320 Hz yield waves oscillating at $f_0=160$ Hz with a wavelength of 2.6 mm. For a dimensionless driving amplitude $\epsilon\equiv(A-A_c)/A_c>0.35$, the pattern is sufficiently disordered that diffusive transport is found [6] (though it is not isotropic at a given instant), and the present measurements are confined to this regime.

In the following sections, we describe the methods used to measure the spatial power spectra and the wave amplitude. Both are needed to determine whether a model based on a fluctuating Stokes drift can account for the dye transport by disordered capillary waves.

A. Spatial power spectra of the surface displacements

We use shadowgraphs for visualization and to estimate the spatial power spectrum semiquantitatively. A collimated beam of light traverses the fluid surface, and is incident on a diffusely scattering Mylar sheet fastened to the top of the cell. A two-dimensional pattern of bright spots is observed on the Mylar sheet due to focusing of the light by the waves. Images are recorded on videotape for analysis. In Fig. 1 we show an example of a shadowgraph for $\epsilon=0.50$, where the waves are partially disordered.

For small ϵ the patterns have square symmetry, and the surface-deformation field (relative to orthogonal axes that may not be well aligned with the container boundaries) is [2,10]

$$h(xy)=A[\cos(k_0x)+\cos(k_0y)]\ . \tag{11}$$

The two-dimensional power spectrum of $h(x,y)$ has peaks at $(k_x,k_y)=(k_0,0)$ and $(0,k_0)$. However, imaging nonlinearities cause the observed intensity distribution to be more complicated, but has been computed by Milner [11]:

$$I(x,y)=b[\cos^2(k_0x)+\cos^2(k_0y)]+c[\cos(k_0x)\cos(k_0y)]+d[\cos^4(k_0x)+\cos^4(k_0y)]+\cdots\ , \tag{12}$$

where b, c, and d are constants which depend on system parameters (wave number, wave amplitude, refractive index, and distance to the screen). The spectral content specified by Eq. (12) can be seen in the experimental power spectra of $I(x,y)$, an example of which is plotted in Fig. 2 using a logarithmic grey scale. The measured spectra are closely related to those of $h^2(x,y)$. To obtain the spectra of $h(x,y)$, the peaks at 45° are first eliminated by using data from a narrow ring, typically 11 pixels wide, that includes the "on-axis" peaks, which are the ones of interest. In addition, they must be shifted from $2k_0$ to k_0, and the square roots of the measured spectra [12] are then used as a better approximation for those of $h(x,y)$. (It is, of course, also necessary to convert from the pixel units of the acquired images to the actual dimensional units. The dominant wave number is $k_0=23.8$ cm^{-1} at $f_0=160$ Hz.)

It is instructive to examine the resulting angular part of $F(k,\theta)$,

$$S(\theta)=\int_{k_0-\Delta k}^{k_0+\Delta k} kF(k,\theta)dk\ ,$$

which is shown in Fig. 3 for the pattern of Fig. 1. The components of $\overleftrightarrow{Q}$ decrease slightly with increasing ϵ, as a result of changes in the wave-number spectrum. However, the variation is only about 30% over the range $0.35<\epsilon<1.57$. We find that $Q_{xx}\approx Q_{yy}\equiv Q$ and

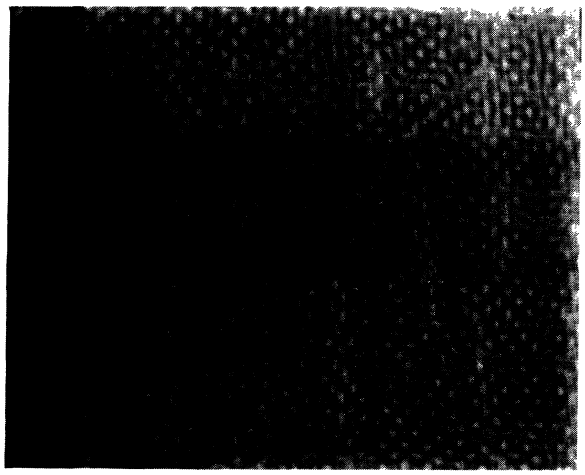

FIG. 1. Shadowgraph of the capillary-wave field at a dimensionless driving amplitude $\epsilon\equiv(A-A_c)/A_c=0.50$, where the pattern is partially disordered.

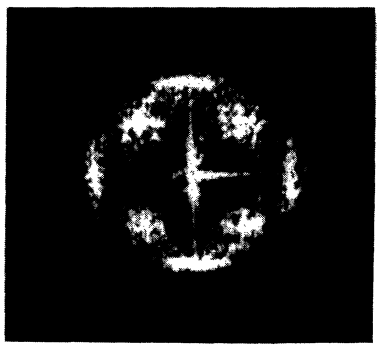

FIG. 2. Spatial power spectrum of the optical-intensity field corresponding to Fig. 1, shown on a logarithmic grey scale. The peaks at 45° are due to an imaging nonlinearity and are removed in the process of estimating the spectrum of $h(x,y)$. The axial peaks correspond to the structure represented by Eq. (11), but are broadened.

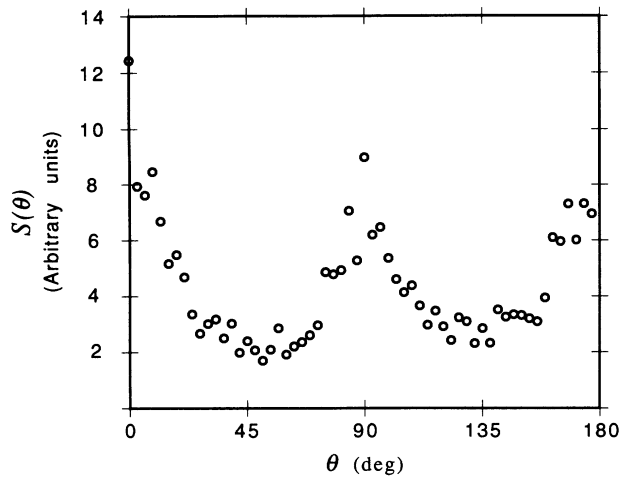

FIG. 3. Angular part $S(\theta)$ of the spatial power spectrum corresponding to the pattern of Fig. 1.

$Q_{xy}=Q_{yx}\approx Q_{xx}/10$. The results indicate that we can describe this diffusion process (for disordered waves) reasonably well by a single diffusion coefficient.

It is difficult to make a quantitative estimate of the uncertainty in Q. However, various tests lead us to the conclusion that the overall error should not be larger than about 40%.

B. Wave amplitudes

To measure the amplitude of the surface waves, we use a laser-beam-deflection technique [13] as illustrated in Fig. 4. A laser beam incident normally on the surface is refracted by the deformed interface. The deflected beam is detected by a position-sensing photodiode (Quantrad PS-200-2) above the cell. Its two output voltages $V_j(t)$ are proportional to the displacements $L_j(t)$ of the beam along the x and y directions, i.e.,

$$V_j(t)=CL_j(t) \ . \tag{13}$$

The relation between the beam displacement and the wave amplitude depends on the particular wave form. In the disordered-wave regime, we approximate the surface waves as sinusoidal waves with wave number k_0, angular frequency ω_0, and slow fluctuating amplitudes and phases:

$$\begin{aligned} h(x,y,t)=&A_{x+}(t)\cos[\omega_0 t+kx+\varphi_+(t)] \\ &+A_{x-}(t)\cos[\omega_0 t-kx+\varphi_-(t)] \\ &+A_{y+}(t)\cos[\omega_0 t+ky+\theta_+(t)] \\ &+A_{y-}(t)\cos[\omega_0 t-ky+\theta_-(t)] \ . \end{aligned} \tag{14}$$

From the geometry in Fig. 4, the displacements may be obtained as follows:

$$\begin{aligned} &\tan\theta_x=\frac{\partial h(x,y,t)}{\partial x} \ , \\ &n\sin\theta_x=\sin\theta_{rx} \ , \\ &L_x=d\tan(\theta_{rx}-\theta_x) \ , \end{aligned} \tag{15}$$

where θ_x is the angle between the laser beam and the normal component to the wave surface in the zx plane, θ_{rx} is the corresponding angle of refraction, n is the index of refraction of the fluid, L_x is the x displacement of the beam, and d is the distance from the mean free surface to the position-sensing photodiode. For small deflection angles, and under the assumption that the amplitude and phase fluctuations are uncorrelated, the mean-square wave amplitude is given by

$$\langle h^2\rangle=\frac{2\langle V_x^2(t)\rangle}{C^2d^2(n-1)^2k_0^2} \ . \tag{16}$$

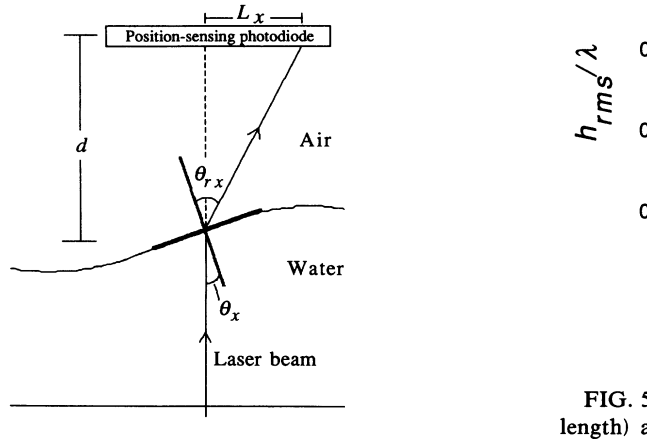

FIG. 4. Geometry of the method used to obtain the mean-square deformation $\langle h^2\rangle$. The xz plane is shown.

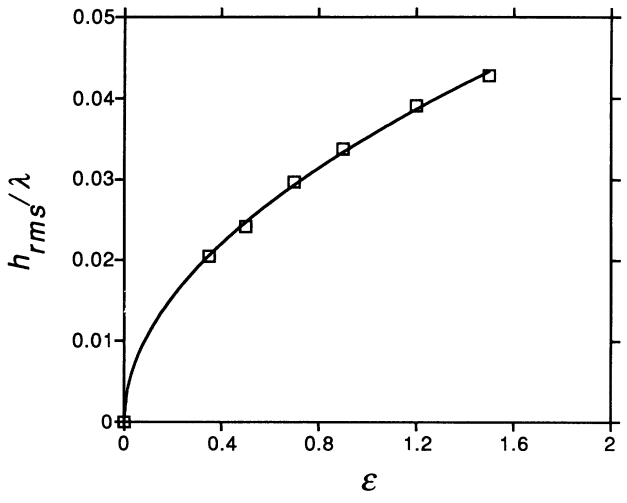

FIG. 5. Measured wave amplitude $h_{\rm rms}$ (in units of the wavelength) as a function of the dimensionless driving amplitude. The variation is well approximated by a power law with exponent 0.51 ± 0.02.

For large wave amplitudes the small-angle approximation is inadequate, and in that case a numerical calibration is employed to obtain $\langle h^2 \rangle$ from the measured values of $\langle v_x^2 \rangle$ and $\langle v_y^2 \rangle$.

We determine $\langle V_x^2 \rangle$ and $\langle V_y^2 \rangle$ using a signal analyzer (HP-3561A). A bandwidth sufficiently large to contain the entire spectral peak is employed to eliminate the need to integrate the spectrum. Even at the highest driving amplitude, harmonics are negligibly small. We find that $\langle V_x^2 \rangle = \langle V_y^2 \rangle$, and that they are independent of the horizontal position of the laser at the surface, so that the random-phase assumption is adequate.

The measured wave amplitude (in units of the wavelength) is displayed as a function of the dimensionless driving amplitude ϵ in Fig. 5. The results are well described by the expression

$$\frac{h_{\rm rms}}{\lambda} = A\epsilon^{\beta} , \tag{17}$$

with $A = 0.035 \pm 0.001$ and $\beta = 0.51 \pm 0.02$.

IV. COMPARISON BETWEEN THEORY AND EXPERIMENT

The vanishing of the off-diagonal components of the angular integral Q_{ij} and the approximate equality of the diagonal terms imply that the calculated diffusion coefficient given by Eq. (6) can be written more simply as

$$D_c = (\pi/6)(T/\rho)^{0.5} \langle h^2 \rangle^2 Q . \tag{18}$$

Since $\langle h^2 \rangle^2$ varies approximately as ϵ^2, and Q depends relatively weakly on ϵ, D_c varies roughly as ϵ^2.

In order to measure the effective-diffusion coefficient for comparison with the model, we we study the dispersion of a fluorescent dye. A small amount of fluorescein powder is placed at one point on the surface and is illuminated with ultraviolet light. The intensity of the fluorescent light is proportional to the local dye concentration. An example of the time evolution of the light-intensity field is shown in Fig. 6. By measuring the evolution of the intensity distribution, the experimental effective-transport coefficient D_m can be quantitatively determined. The method has been thoroughly discussed by Ramshankar and Gollub [6].

In Fig. 7 the "calculated" and measured values D_c and D_m are displayed as a function of the normalized wave amplitude. (We use quotes around the word "calculated" because *measurements* of spatial power spectra are required for these estimates.) The measured transport is

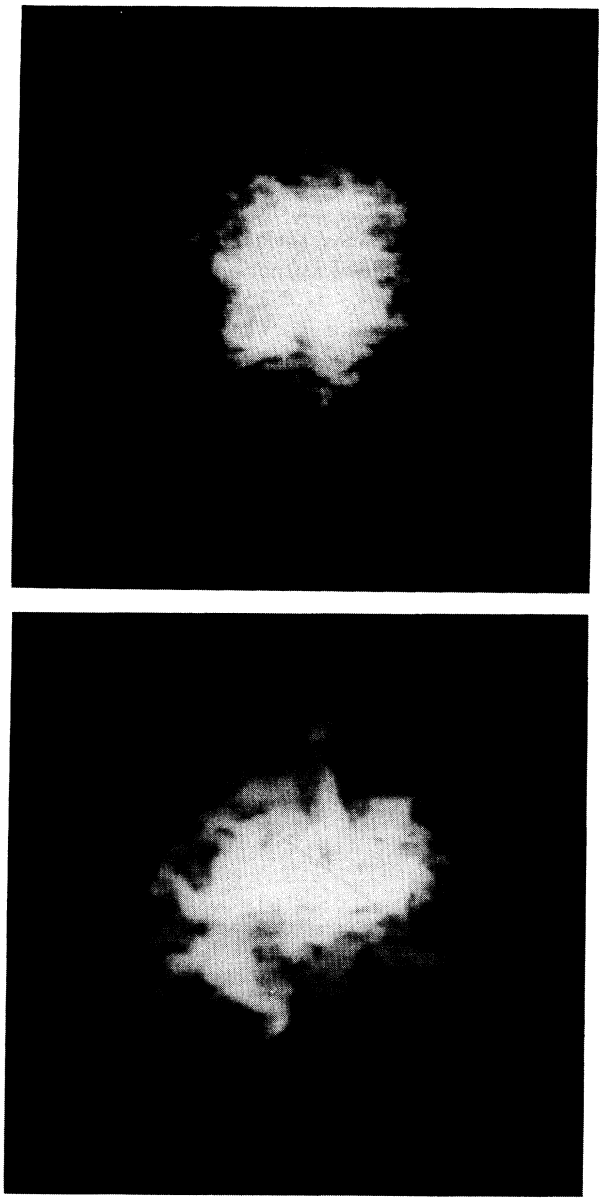

FIG. 6. Fluorescein-dye patch dispersal for $\epsilon = 0.90$. These optical-intensity distributions were obtained 2 and 4 s after the dye was introduced onto the surface.

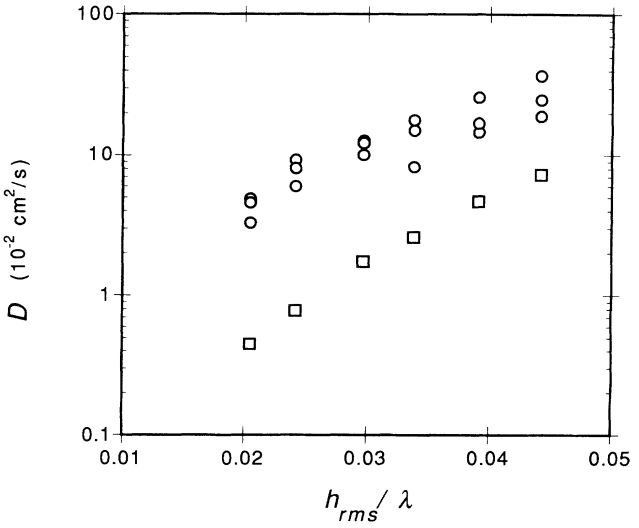

FIG. 7. Test of the fluctuating Stokes-drift model of capillary-wave transport: measured and calculated effective-diffusion coefficients (D_m, circles; D_c, squares) as a function of the nondimensional wave amplitude.

somewhat faster than the model would lead one to expect, but the discrepancy declines with increasing ϵ. At the upper end of the investigated range, the measured transport is about a factor of 3 faster than the "calculated" values.

The fluctuating Stokes-drift model thus gives a sufficient mechanism to account for the existence of substantial transport. The excess transport may be a result of one or more of the following: (a) The waves are more strongly spatially correlated than the model assumes; (b) approximations in measuring $\langle h^2 \rangle$ or Q are inadequate; or (c) there is, in addition, some other mechanism of transport, such as large-scale flows induced by the lateral boundaries. (We believe that such large-scale flows are unimportant here, but is is difficult to provide clear proof.)

Since the calculated diffusion coefficients vary with the fourth power of the root-mean-square amplitude $h_{\rm rms}$, an error of only 40% in the latter could account for the entire difference between D_c and D_m. Therefore, we are inclined to regard the fluctuating Stokes-drift model as basically adequate to describe transport for *disordered* waves at large ϵ. The case of small ϵ, where the waves are ordered but modulated, remains to be understood quantitatively.

ACKNOWLEDGMENTS

This work has been supported by National Science Foundation Grant No. DMR-8901869 and by the University Research Initiative program under Contract No. DARPA/ONR N00013-85-K-0759. We acknowledge T. Davis for experimental assistance. O.N.M. acknowledges partial support from the Brazilian Agency Conselho Nacional de Desenvolvimento Cientifico e Tecnologico (CNPq).

*Permanent address: Departamento de Física, Universidade Federal de Minas Gerais, Belo Horizonte, MG 31270, Brazil.

[1] J. Miles and D. Henderson, Annu. Rev. Fluid Mech. **22**, 143 (1990).

[2] J. P. Gollub and R. Ramshankar, in *New Perspectives in Turbulence,* edited by S. Orszag and L. Sirovich (Springer-Verlag, Berlin 1991).

[3] J. P. Gollub, Physica D **51**, 501 (1991).

[4] N. B. Tufillaro, R. Ramshankar, and J. P. Gollub, Phys. Rev. Lett. **62**, 422 (1989).

[5] For example, see Proceedings of the Conference on the Fluid Mechanics of Stirring and Mixing, edited by H. Aref [Phys. Fluids A **3**, 723 (1991)].

[6] R. Ramshankar, D. Berlin, and J. P. Gollub, Phys. Fluids A **2**, 1955 (1990); R. Ramshankar and J. P. Gollub, *ibid.* **3**, 1344 (1991).

[7] I. S. Aranson, A. B. Ezersky, M. I. Rabinovich, and L. Sh. Tsimring, Phys. Lett. **153A**, 211 (1991).

[8] K. Herterich and K. Hasselmann, J. Phys. Oceanog. **12**, 704 (1982).

[9] J. Lighthill, *Waves in Fluids* (Cambridge University Press, Cambridge, England, 1979).

[10] S. T. Milner, J. Fluid Mech. **225**, 81 (1991).

[11] S. T. Milner (private communication).

[12] For Gaussian line shapes, the square root of the measured intensity spectrum gives the spectrum of $h(x,y)$. However, the final results for D_c are not sensitive to whether or not this operation is performed (the difference is about 20%), provided that the normalization given by Eq. (3) is maintained.

[13] For example, see J. P. Gollub and C. W. Meyer, Physica D **6**, 337 (1983).

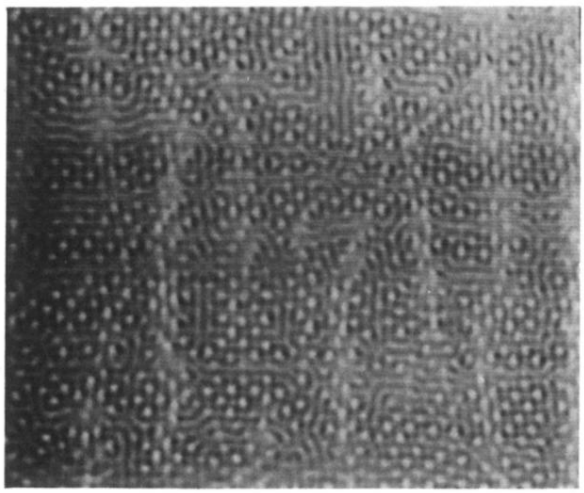

FIG. 1. Shadowgraph of the capillary-wave field at a dimensionless driving amplitude $\epsilon \equiv (A - A_c)/A_c = 0.50$, where the pattern is partially disordered.

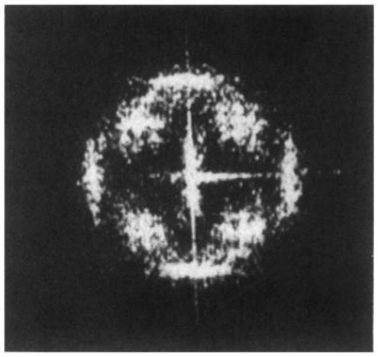

FIG. 2. Spatial power spectrum of the optical-intensity field corresponding to Fig. 1, shown on a logarithmic grey scale. The peaks at 45° are due to an imaging nonlinearity and are removed in the process of estimating the spectrum of $h(x,y)$. The axial peaks correspond to the structure represented by Eq. (11), but are broadened.

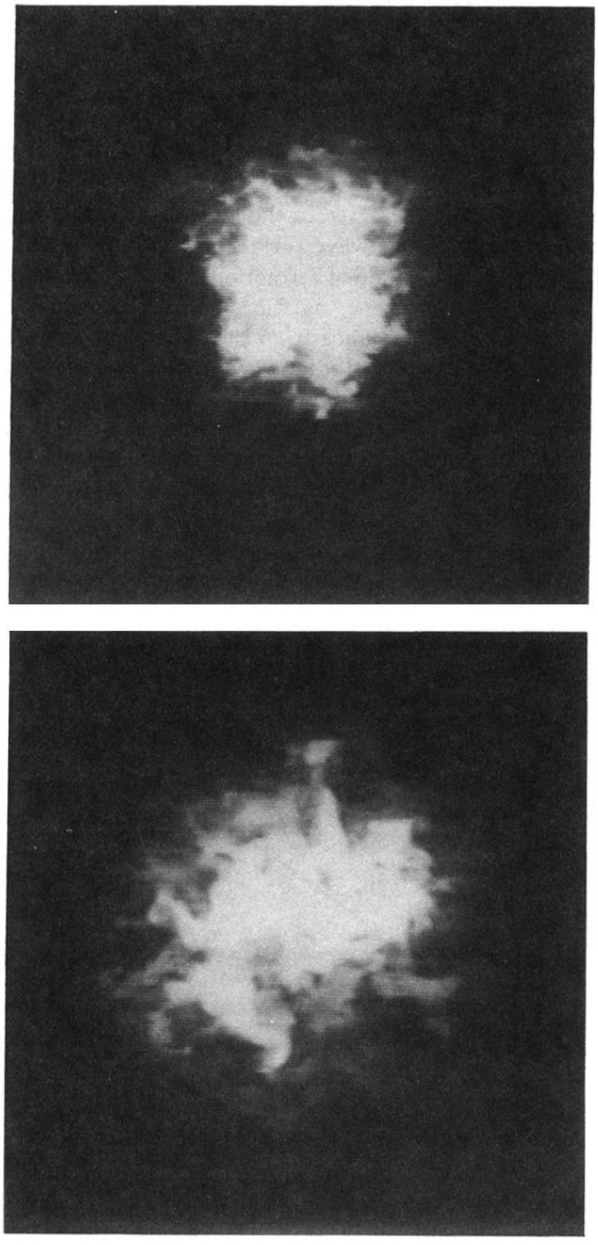

FIG. 6. Fluorescein-dye patch dispersal for $\epsilon=0.90$. These optical-intensity distributions were obtained 2 and 4 s after the dye was introduced onto the surface.